Full-wave Rectified Waveform Generation Using Dead-beat Voltage Control for DC-DC Buck Converters to Realize High Efficiency Inverter

Sakahisa Nagai, Satoshi Nakazaki, Shogo Ito, Hidemine Obara, and Atsuo Kawamura
YOKOHAMA NATIONAL UNIVERSITY
79-5, Tokiwadai, Hodogaya-ku
Yokohama, Japan
Tel.: +81 / (45) – 339 – 4162
E-Mail: (nagai-sakahisa-yf, nakazaki-satoshi-rj, ito-shogo-wr)@ynu.jp,
(obara-hidemine-mh, kawamura)@ynu.ac.jp

Keywords

«Converter control», «Digital control», «Voltage source inverters (VSI)»

Abstract

This study aims to realize a high efficiency inverter by combining a DC-DC buck converter and unfolding circuit. The DC-DC converter generates a full-wave rectified waveform. The unfolding circuit changes the waveform to an AC sinusoidal waveform. In order to generate a pure AC voltage waveform, the output of the DC-DC converter should be accurately controlled. In this paper, dead-beat voltage control (DBVC) for the accurate full-wave rectified waveform generation is proposed. Simulations and experiments were conducted to validate the proposed method. As a result, it was verified that the proposed DBVC was effective for the accurate full-wave rectified waveform generation. A voltage distortion was observed when the voltage reference was close to zero. In order to suppress the distortion, only the duty after the voltage reference turns to increase is decreased. As the improved results, the distortion can be reduced by setting the decrease ratio of the duty at 0.6. Finally, the AC output waveform with low harmonics was achieved by combining the DC-DC converter and the unfolding circuit.

Introduction

Power conversion systems for automotive applications are actively studied all over the world [1]-[4]. In order to extend one charge traveling distance, power converters with high efficiency, high power density, and light weight are necessary. In [1], a dual active bridge converter for automotive applications was developed. In [2], a DC-DC converter based on partial power converter concept with two batteries was proposed to realize high efficiency power conversion. S. Dusmez et. al. have conducted a comparison of bidirectional three-level DC-DC converters for the automotive applications [3]. These power conversion technologies with high efficiency and high power density are useful for not only the automotive applications but also other applications such as poser conditioners for photovoltaic generation, power supplies for data centers, and so on.

This study aims to realize a high efficiency DC-AC inverter. Fig. 1 shows the concept of the system, which consists of a high efficiency DC-DC buck converter and an unfolding circuit [5].

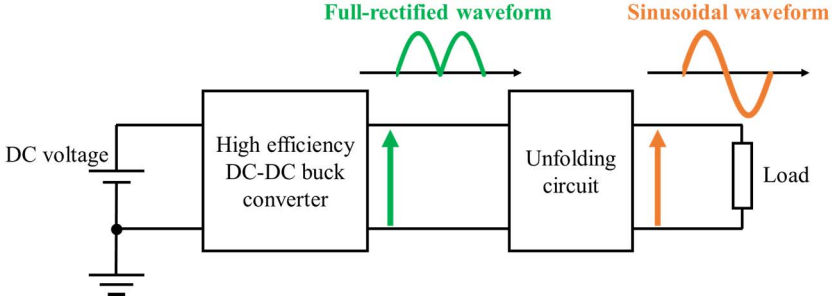

Fig. 1: Concept of high efficiency DC-AC inverter

The DC-DC buck converter generates a full-wave rectified waveform with high efficiency. The waveform is converted to a sinusoidal waveform by the unfolding circuit.

This paper focuses on the full-wave rectified waveform generation by the DC-DC buck converter. The accuracy of the output voltage waveform is important to generate a clean sinusoidal wave. However, the full-wave rectified waveform is a discontinuous waveform. In order to generate the precise waveform, accurate and quick voltage control is required especially at the instant when the voltage increases from zero.

Various control methods for the buck DC-DC converters have been proposed [6]-[9]. In this paper, a dead-beat voltage control (DBVC) is utilized since the output voltage can be directly controlled [10], [11]. Simulations and experiments are conducted to verify the effectiveness of the DBVC for the generation of the full-wave rectified waveform.

This paper is organized as follows: Firstly, the modeling of the DC-DC buck converter is explained. Next, the DBVC law based on the discrete model of the DC-DC buck converter is described. The simulation results and the experimental results are shown. Finally, the conclusions are described.

Modeling of DC-DC Buck Converter

This section describes a modeling of the DC-DC buck converter. Fig. 2 shows the circuit diagrams of the high efficiency buck converter.

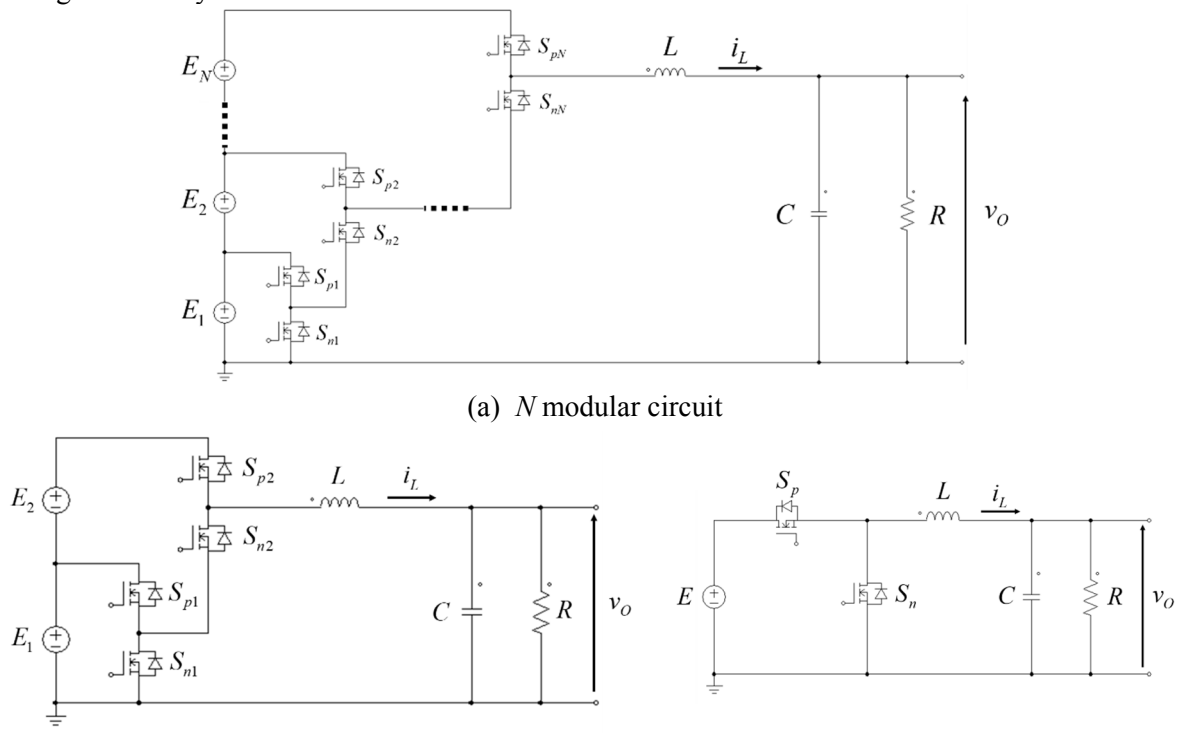

(a) N modular circuit

(b) Two modular circuit.

(c) Simplest one modular circuit (general buck converter)

Fig. 2: DC-DC buck converter circuit

The number of the series connected DC-DC converters can be extended as shown in Figs. 2(a) and (b). This chapter focuses on the full-wave rectified waveform generation by the DC-DC converter. Therefore, the simplest one modular buck converter shown in Fig. 2(c) is dealt with. E, L, C, and R denote the input DC voltage, filter inductance, filter capacitance, and load resistance, respectively as shown in Fig. 2(c). S_p and S_n are the MOSFET switches. v_O and i_L are the output voltage and inductor current. The state equation of the DC-DC buck converter is expressed as

$$\dot{\boldsymbol{x}}(t) = \boldsymbol{A}\boldsymbol{x}(t) + \boldsymbol{B}u(t) \tag{1}$$

where t denotes the time. The state variable $\boldsymbol{x}(t)$ and input $u(t)$ are defined as

$$\boldsymbol{x}(t)=\begin{bmatrix} v_O(t) \\ i_L(t) \end{bmatrix}, \qquad u(t)=E. \tag{2}$$

The state matrix $\boldsymbol{A}$ and the input matrix $\boldsymbol{B}$ are expressed as

$$\boldsymbol{A}=\begin{bmatrix} -1/CR & 1/C \\ -1/L & 0 \end{bmatrix}, \qquad \boldsymbol{B}=\begin{bmatrix} 0 \\ 1/L \end{bmatrix}. \tag{3}$$

The discrete model of (1) can be calculated as

$$\boldsymbol{x}[k+1]=\boldsymbol{F}\boldsymbol{x}[k]+\boldsymbol{G}\Delta T[k] \tag{4}$$

where

$$\boldsymbol{x}[k]=\begin{bmatrix} v_O[k] \\ i_L[k] \end{bmatrix}. \tag{5}$$

$\Delta T\,[k]$ is the on-state time of the switch S_p. The matrices $\boldsymbol{F}$ and $\boldsymbol{G}$ are calculated as

$$\boldsymbol{F}=e^{AT}=\begin{bmatrix} F_{11} & F_{12} \\ F_{21} & F_{22} \end{bmatrix}, \qquad \boldsymbol{G}=e^{AT/2}\boldsymbol{B}E=\begin{bmatrix} g_1 \\ g_2 \end{bmatrix}. \tag{6}$$

Here, T denotes the switching period.

Dead-beat Voltage Control (DBVC)

Derivation of DBVC Law

This section describes a DBVC law for the DC-DC buck converters [10], [11]. From the discrete model in (4), the voltage equation can be rewritten as

$$v_O[k+1]=F_{11}v_O[k]+F_{12}i_L[k]+g_1\Delta T[k]. \tag{7}$$

By replacing $v_O[k+1]$ with the reference voltage v_{ref} and solving (7) into $\Delta T\,[k]$, the DBVC law can be derived as

$$\Delta T[k]=\frac{1}{g_1}\left(v_{ref}-F_{11}v_O[k]-F_{12}i_L[k]\right). \tag{8}$$

State Observer

This section describes a state observer. In this paper, a digital signal processor (DSP) controller is used. The DSP takes one switching period from the sampling of the output voltage and inductor current to the reference updating. In other words, the calculated $\Delta T\,[k]$ cannot be applied immediately after the calculation. Therefore, the $\Delta T\,[k]$ is input to the switch with one sample delay. In order to compensate this delay, the state observer is utilized.

The state variable can be estimated as

$$\hat{\boldsymbol{x}}[k+1]=\boldsymbol{F}\hat{\boldsymbol{x}}[k]+\boldsymbol{G}\Delta T[k]+\boldsymbol{K}\left(\boldsymbol{x}[k]-\hat{\boldsymbol{x}}[k]\right) \tag{9}$$

where $\boldsymbol{K}$ is the observer gain matrix. The symbol with '^' means estimated value. In the DBVC law described in (8), the estimated values in (9) are used instead of the measured values. The block diagram of the controller is shown in Fig. 3.

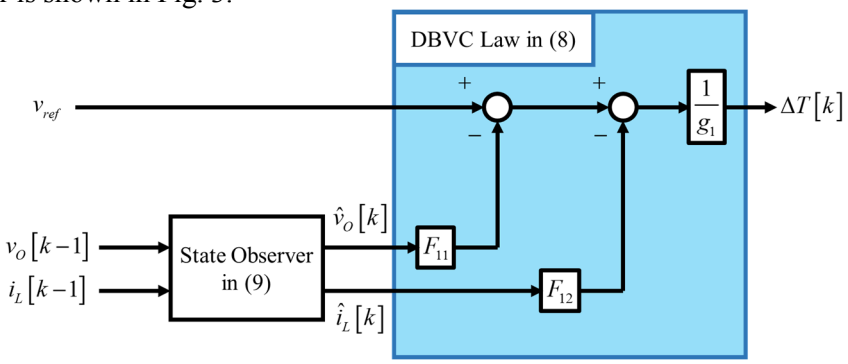

Fig. 3: Block diagram of DBVC controller

Simulations

This section describes simulation results of the DBVC. The simulations were conducted to confirm the effectiveness of the DBVC by PSIM produced by Powersim Inc. Additionally, the responses of an asynchronous rectifier converter and a synchronous rectifier converter were compared in this simulation. This means that the low-side MOSFET S_n shown in Fig. 2(c) is operated as the free-wheeling diode in the former case and switch in the latter case.

The state observer explained in the last subsection was utilized. The observer gain matrix $\boldsymbol{K}$ was decided by placing the pole of the matrix ($\boldsymbol{F} - \boldsymbol{K}$) at 0.4 (multiple root).

This paper focuses on the generation of the full-wave rectified waveform. The reference voltage v_{ref} was set as

$$v_{ref} = \overline{v}\left|\sin\left(2\pi ft\right)\right| \tag{10}$$

where $\overline{v}$ and f denote the amplitude and frequency of the waveform, respectively.

The parameters used in the simulations are shown in Table I. Figs. 4 and 5 show the responses of the asynchronous rectifier converter and the synchronous rectifier converter, respectively.

Table I: Parameters

Input DC voltage	E	100 V
Inductor	L	585 µH
Capacitor	C	80 µF
Load resistor	R	10 Ω
Switching frequency	$1/T$	20 kHz
Amplitude of v_{ref}	$\overline{v}$	50 V
Frequency of v_{ref}	f	50 Hz

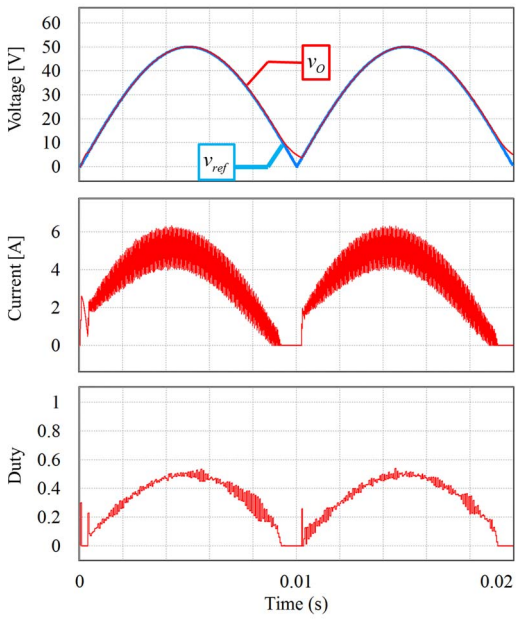

Fig. 4: Simulation results of asynchronous rectifier converter (Top: Voltage, Middle: Current, Bottom: Duty)

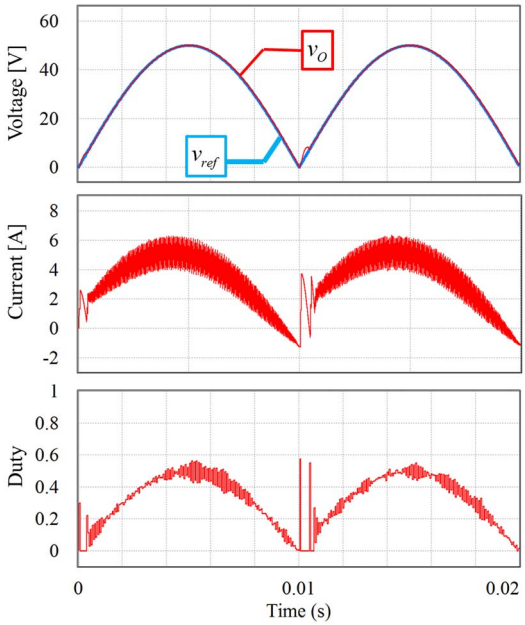

Fig. 5: Simulation results of synchronous rectifier converter (Top: Voltage, Middle: Current, Bottom: Duty)

The top, middle, and bottom figures in each figure show the output voltage response, inductor current, and duty signal, respectively. From Figs. 4 and 5, it was confirmed that the output voltage of both converters followed the reference value v_{ref}. However, there is difference in the voltage response when v_{ref} is small. Fig. 6 shows the enlarged view of the voltage response of Figs. 4 and 5 when v_{ref} is small.

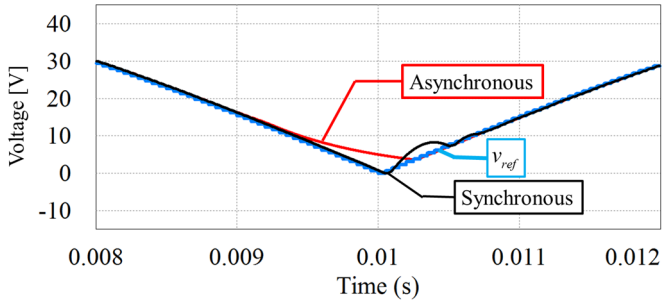

Fig. 6: Enlarged view of voltage response when v_{ref} is small

As the result, it is observed that the asynchronous converter cannot output voltage less than about 5 V. From the current response of the asynchronous converter, the discontinuous mode can be observed, because the current direction of the inductor cannot be negative. On the other hand, the synchronous rectifier converter can output small voltage because the current continuously flows bidirectionally.

Experiments

This section describes experimental setup and results. The experiments were conducted to confirm the effectiveness of the DBVC for the full-wave rectified waveform generation. Moreover, a generation of the sinusoidal output waveform is demonstrated by using both the DC-DC converter with the DBVC and unfolding circuit as shown in Fig. 1.

Experimental setup

Figs. 7 and 8 show the experimental system and the photograph of the experimental setup, respectively. The digital processing system PE-Expert4 produced by Myway Plus Corp. was used as a controller for the DBVC. The main controller is a DSP. The inductor current was measured by using the current sensor "LAX 100-NP" produced by LEM. The output voltage was measured using the isolation amplifier

"AD215BY" produced by Analog Devices. The experimental parameters are the same with the simulation conditions listed in Table I. In the experiments, a synchronous rectified converter was used. The dead time was set at 500 ns, which is 1 % of the switching period.

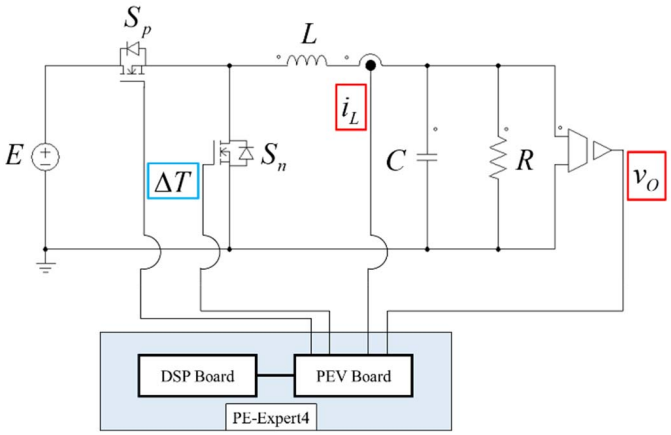

Fig. 7: Experimental system

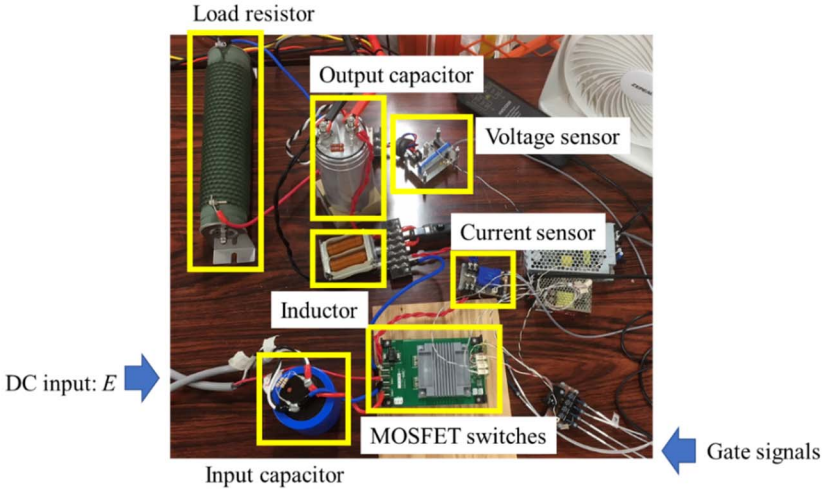

Fig. 8: Photograph of experimental setup

Experimental results

Fig. 9 shows the experimental results of the full-wave rectified wave generation by the DBVC.

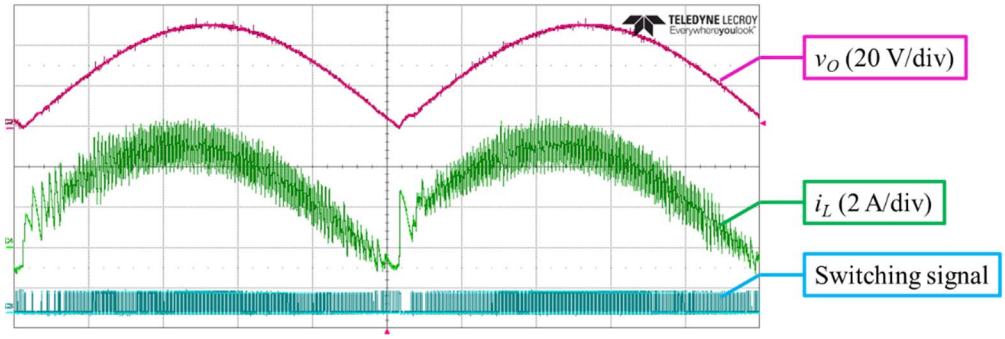

Fig. 9: Experimental results of the full-wave rectified wave generation (2.0 ms/div)

The top, middle, and bottom lines show the output voltage response, inductor current, and switching signal of S_p, respectively. The waveforms were measured by using the oscilloscope "Wavesurfer 3024" produced by TELEDYNE LECROY. From the experimental results, it was confirmed that the output voltage was adequately controlled to the full-wave rectified waveform. Fig. 10 shows the output voltage response when the reference voltage v_{ref} was small. The waveform is very similar to the simulation result

in Fig. 6. However, there is small distortion when the voltage reference turns to increase. In order to generate the accurate voltage waveform, the distortion should be suppressed.

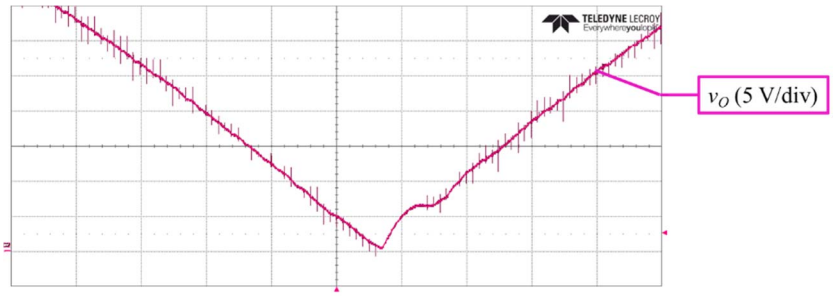

Fig. 10: Voltage response when v_{ref} is small (500 μs/div)

Suppression of distortion in output voltage

A small distortion of the output voltage was observed when the voltage reference switches from the decrease to increase. From Fig. 8, the calculated duty at around 0.01 s is about 0.3. After the duty of 0.3, the duty becomes 0.0 during a few samples because the output voltage is larger than the reference. In short, the reason why the distortion occurred is that the calculated duty when the voltage reference switched from decrease to increase is a little large.

In order to suppress the distortion, only the duty after the voltage reference turns to increase should be decreased. Fig. 11 shows the comparison of the output voltage responses with change of the decrease ratio when the voltage reference is small.

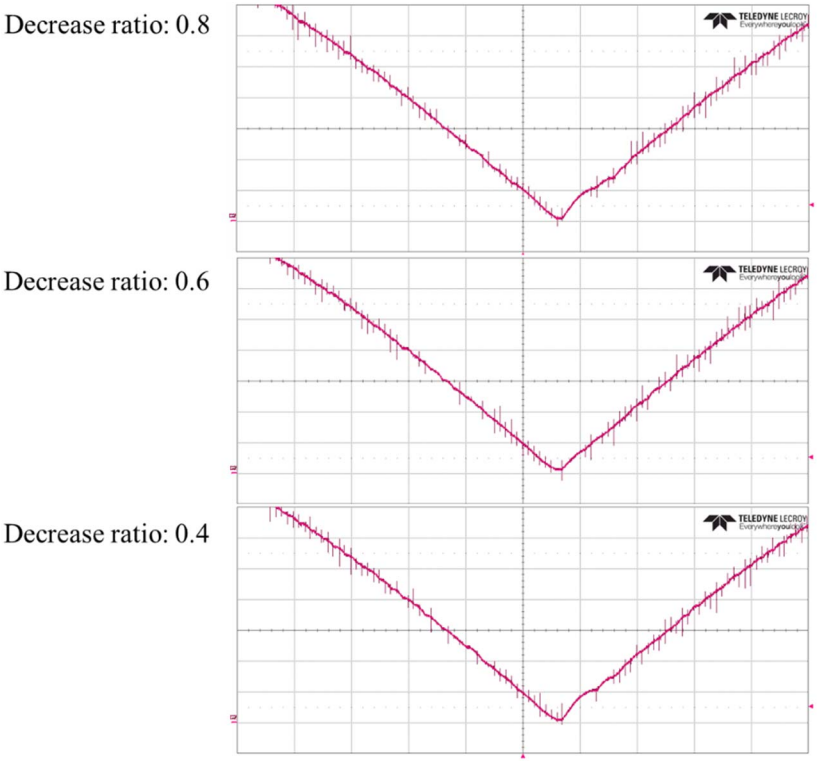

Fig. 11: Comparison of output voltage responses with change of decrease ratio when v_{ref} is small (5.0 V/div, 500 μs/div)

The decrease ratio means how much the duty after the voltage reference turns to increase is decreased. Therefore, the result when the decrease ratio is 1.0 is the same response as shown in Fig. 10. As the result, when the decrease ratio was set at 0.6, the distortion could be suppressed successfully. On the other hand, the distortion was observed even when the decrease ratio was set as smaller at 0.4. Hence, the distortion occurs when the decrease ratio is too large or too small.

AC output by unfolding circuit

This subsection describes the experimental results of the AC output by the additional unfolding circuit. The load resistor in Fig. 7 is replaced with the unfolding circuit and load resistor as shown in Fig. 12. Two IGBT modules are used for the H-bridge configuration.

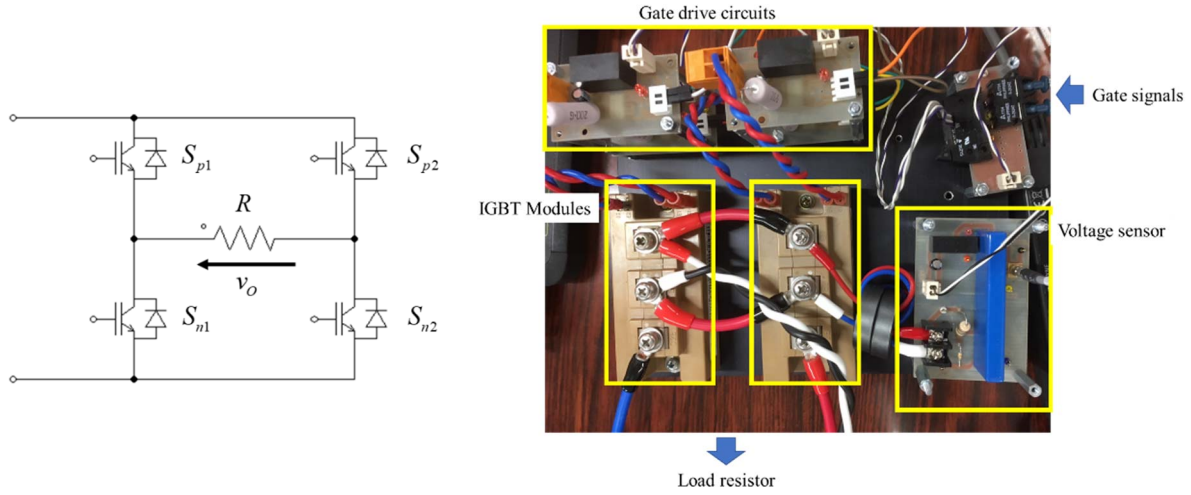

Fig. 12: Unfolding circuit (Left: Circuit diagram, Right: Photograph)

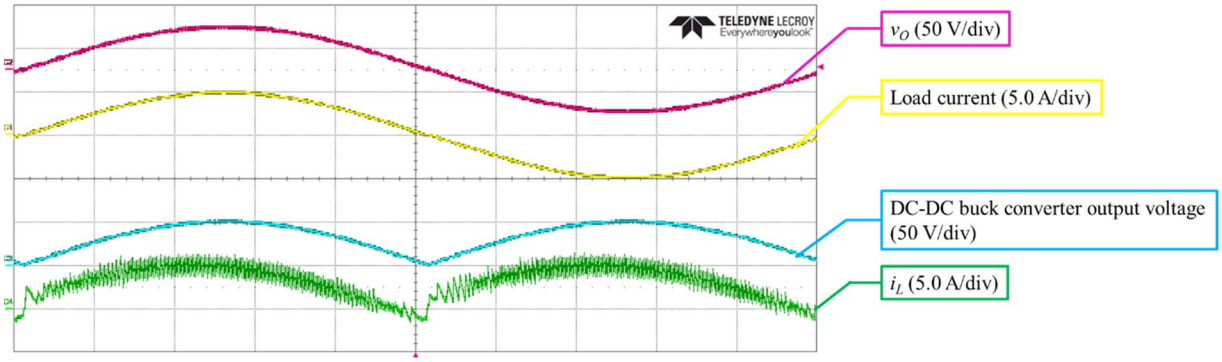

Fig. 13: Experimental result of AC output by unfolding circuit (2.0 ms/div)

The switch states of the IGBTs (S_{p1}, S_{n1}) and (S_{p2}, S_{n2}) are changed at the instant when the reference voltage v_{ref} becomes zero. Fig. 13 shows the experimental result of the AC output by combining the DC-DC converter generating the full-wave rectified waveform and the unfolding circuit. The decrease ratio was set at 0.6. As the result, it was verified that the converter with the proposed DBVC could output a clean AC voltage waveform.

Conclusions

This paper proposed full-wave rectified waveform generation using DBVC for DC-DC buck converters. The reference of the full-wave rectified waveform has discontinuity. Therefore, the DBVC is effective so that the output voltage quickly follows the reference voltage. Simulations and experiments were conducted to confirm the followability of the DBVC. As the experimental results, it has been confirmed that the output voltage quickly followed the full-wave rectified waveform reference. However, a small distortion was observed when the voltage reference switched from the decrease to increase. As the result applying the improved method, it has been confirmed that the distortion could be reduced by setting the decrease ratio of the duty at 0.6. Finally, the clean AC voltage output has been achieved by combining the DC-DC converter with the DBVC and unfolding circuit.

References

[1] F. Krismer and J. W. Kolar: Efficiency-optimized high-current dual active bridge converter for automotive applications, IEEE Trans. Ind. Electron. Vol. 59 no. 7, pp 2745- 2760, Jul. 2012

[2] Y. Tsuruta and A. Kawamura: Principle verification prototype chopper using SiC MOSFET module developed for partial boost circuit system, in Proc. of IEEE Energy Conversion Congress and Exposition, Sept. 2015

[3] S. Dusmez, A. Hasanzadeh, and A. Khaligh: Comparative analysis of bidirectional three-level DC-DC converter for automotive applications, IEEE Trans. Ind. Electron. Vol. 62 no 5, pp 3305- 3315, May 2015

[4] K. Aoyama, N. Motoi, Y. Tsuruta, and A. Kawamura: High efficiency energy conversion system for decreases in electric vehicle battery terminal voltage, IEEJ Journal of Industry Applications, Vol. 5 no. 1, pp 12-19, 2016

[5] Y. Lei, C. Barth, S. Qin, W.-C. Liu, I. Moon, A. Stillwell, D. Chou, T. Foulkes, Z. Ye, Z. Liao, and Robert C.N. Pilawa-Podgurski: A 2 kW, single-phase, 7-level, GaN inverter with an active energy buffer achieving 216~W/in3 power density and 97.6 % peak efficiency, in Proc. of IEEE Applied Power Electronics Conference and Exposition, Mar. 2016

[6] J.-S. Chang, H.-S. Oh, Y.-H. Jun, and B.-S. Kong: Fast output voltage-regulated PWM buck converter with an adaptive ramp amplitude control, IEEE Trans. Circuits and Systems Vol. 60 no. 10, pp 712- 716, Oct. 2013

[7] S. Bibian and H. Jin: High performance predictive dead-beat digital controller for DC power supplies, IEEE Trans. Power Electronics Vol. 17 no 3, pp 420- 427, May 2002

[8] S. Saggini, W. Stefanutti, E. Tedeschi, and P. Mattavelli: Digital deadbeat control tuning for dc-dc converters using error correlation, IEEE Trans. Power Electronics Vol. 22 no 4, pp 1566- 1570, Jul. 2007

[9] D. Maksimovic and R. Zane: Small-signal discrete-time modeling of digitally controlled PWM converters, IEEE Trans. Power Electronics Vol 22 no 6, pp 2552- 2556, Nov. 2007

[10] A. Kawamura, T. Hanegishi, R. G. Hoft: Deadbeat controlled PWM inverter with parameter estimation using only voltage senser, IEEE Trans. Power Electronics Vol. 3 no 2, pp 118- 125, Apr. 1988

[11] K. P. Gokhale, A. Kawamura, R. G. Hoft: Dead beat microprocessor control of PWM inverter for sinusoidal output waveform synthesis, IEEE Trans. Ind. Appl. Vol. IA-23 no 5, pp 901- 910, Sept. 1987